Composite cathode prepared by argyrodite precursor solution assisted by dispersant agents for bulk-type all-solid-state batteries

Nataly Carolina Rosero-Navarro*, Akira Miura and Kiyoharu Tadanaga

Division of Applied Chemistry, Faculty of Engineering, Hokkaido University, Sapporo 060-8628, Japan

Corresponding Author

*E-mail address: rosero@eng.hokudai.ac.jp

Abstract

All-solid-state lithium batteries based on sulfide solid electrolytes are potential candidates for large-scale energy storage applications. Here, composite cathode with high content of an active material was prepared by a liquid phase process assisted by a dispersant agent to produce a better electrode and electrolyte interface. Li_6PS_5Cl sulfide electrolyte derived from a solution containing dispersant showed an argyrodite crystal phase with a better distribution of particle size and higher conductivity compared with those without dispersant. Regular distribution of Li_6PS_5Cl particles in nanometric scale with a spherical shape below 500 nm and conductivity of 0.6 x 10^{-3} S cm^{-1} (ρ = 1.40 g cm^{-3}) at room temperature were obtained. Composite cathode was prepared by the dispersion of $LiNi_{1/3}Mn_{1/3}Co_{1/3}O_2$ particles and carbon additive in the Li_6PS_5Cl-solution containing dispersant agent and subsequent drying at 180 ºC. Bulk-type all-solid-state battery fabricated with the composite cathode containing 89 wt% of the active material showed an initial discharge capacity of 110 mA h g^{-1} at 25 ºC and maintained 95% discharge capacity after 15 cycles.

Introduction

All-solid-state lithium batteries (ASLBs) are potential candidates for large-scale energy storage applications such as electrical vehicle and smart grids. The solid electrolytes (SEs) have proven to be electrochemically and thermally stable, making them suitable to be operated at high voltages and/or elevated temperatures [1]. Sulfide-based solid electrolytes (SSEs) have been widely used to fabricate bulk-type ASLBs [2-5], because of their high conductivity (10^{-2}–10^{-4} S cm^{-2}) and sound mechanical properties (young's modulus of 20 – 40 GPa) [6, 7]. Typically, ASLBs based on SSE are fabricated by only cold pressing, using composite cathode contains solid electrolyte and/or carbon additives to improve ionic and electronic conduction to the active material [2-5].The amount of solid electrolyte in the composite cathode is crucial to obtain a low interfacial electrode/electrolyte resistance, however, large amount limits the total energy density. ASLBs with composite cathode prepared with a SSE amount of 30 - 60 wt% achieve up to 70% of the total theoretical discharge capacity (e.g. circa of 100 mA h g^{-1} for $LiCoO_2$ [2, 3]).

Higher energy density requires the reduction of solid electrolyte content in the composite cathode. Ideally, a high content of active material of around ~90% or higher, is a desired target. In this regard, an adequate distribution of each component through the composite cathode layer is the major drawback. SSE-layer deposited on active materials, such as $LiCoO_2$ and $LiNi_{1/3}Mn_{1/3}Co_{1/3}O_2$ (NMC) particles, by pulsed

laser deposition (PLD) [8, 9] or liquid phase process [10-16] have been evaluated to produce lower interfacial electrode/electrolyte resistances. The SSE amount has been significantly reduced by PLD process. The preparation of composite cathode using $LiCoO_2$ and rather low amount of SSE-layer around 3 wt% with a thickness of approximately 200 nm (Li_4GeS_4-Li_3PS_4, 1.8 x 10^{-3} S cm^{-1}) by PLD process has recently been reported [9]. The bulk-type ASLB fabricated with this composite cathode displayed a discharge capacity of up to 80 mA h g^{-1}. The good electrochemical performance of the battery has been explained by the effective formation of a thin and homogenous SSE-layer on the active material particles.

The liquid phase process has also proven to be an effective and simple process to form favorable interfaces since the SSE-solution can cover the solids particles and then after solvent removal creates a SSE-layer. However, the composite cathode prepared by liquid phase process needs slightly higher SSE amount, compared with PLD process, to warrantee a sufficient lithium conduction at the electrode/electrolyte interface. The preparation of composite cathodes by liquid phase process have been reported using $LiCoO_2$ or NMC and c.a. 15 wt% SSE-layer. SSEs with high conductivity of 10^{-4} – 10^{-5} S cm^{-1} have been reported from different solvents such as methanol [12], water [13] or solvent mixture, ethanol and ethyl propionate [14]. The composite cathodes have been prepared after solvent removal at 180 ºC – 200 ºC [12, 14] or higher temperature at 320 ºC [13] to promote higher ionic conductivity of SSE-layer. Bulk-type ASLBs fabricated with these composite cathodes (15 wt% SSE) have achieved good electrochemical properties, verified by the high initial

discharge capacities of 110 - 120 mA h g^{-1}. The effort to reduce the amount of SSE-layer (<10 wt%) into the composite cathode by liquid phase process, to increase the total energy density, inevitably leads to a drop of the discharge capacity. Initial discharge capacities between 30 and 45 mA h g^{-1} [15, 16] have been reported from bulk-type ASLBs prepared with composite cathode using $LiCoO_2$ or NMC and 7.5 - 10 wt% Li_6PS_5Cl-layer (~10^{-5} S cm^{-1}, precipitated from ethanol solution). The unsatisfactory electrochemical performance of these batteries can be associated with a scarce covering of SSE-coating layer on active material and/or the low conductivity of the sulfide-solid electrolytes obtained by liquid phase process. Recently, Matsuda et al.[17] satisfactorily prepared a composite cathode with a low content of SSE (10 wt%) using a Li_3PS_4 nanoplates (2 x 10^{-4} S cm^{-1}). The ASLB cell achieved an initial discharge capacity up to 130 mA h g^{-1}. The nanostructuring of SSE-layer could be a potential alternative to producing a better electrode/electrolyte interface, thus improving the battery performance.

The preparation of composite cathode by using liquid phase process with low content of sulfide solid electrolyte (<10 wt%) is challenging. It could be more technologically (and economically) suitable to an industrial scale-up. The aim of the present work is to prepare a composite cathode with a low content of SSE by liquid phase process, assisted by a dispersant agent. Our approach involves the strategic selection of protic/aprotic solvents and dispersant to overcome the expected drawbacks associated with the insufficient covering of SSE- layer on active material. Acetonitrile is a feasible alternative as a solvent since it has proven to play a surfactant role in

the synthesis of sulfide solid electrolyte leading to the precipitation of particles in the nanometric scale and high ionic conductivity of up to ~10^{-3} S cm^{-1} [18, 19]. The adequate ethanol content was used to produce a complete dissolution of SSE. Moreover, a commercially available dispersant Triton X-100 was used to control the precipitation of the SSE during solvent removal and further to achieve a better electrode/electrolyte interface.

High ionic conductor solid electrolyte argyrodite-type Li_6PS_5Cl and high voltage cathode $LiNi_{1/3}Mn_{1/3}Co_{1/3}O_2$ were used as a reference system to prepare the composite cathode by liquid phase process as this system had been prepared by the same process using ethanol as a solvent [15, 16].

Experimental

Synthesis of composite cathode

The Li_6PS_5Cl solid electrolyte was firstly prepared by mechanical milling process following a procedure reported previously [16]. Typically, 0.5 g of stoichiometric proportions of Li_2S (Mitsuwa's Purity Chemicals, 99.9%), P_2S_5 (Sigma Aldrich, 99%) and LiCl (Sigma Aldrich, 99.9%) were milled with 15 zirconia balls (10 mm diameter) in a zirconia pot (45 mL) using a planetary ball mill (PULVERISETTE, Fritsch, Germany) for 40 h at 600 RPM. The as-synthetized Li_6PS_5Cl solid electrolyte powder with an ionic conductivity of 4 x 10^{-5} S cm^{-1} was then used to prepare the SSE-solution and further, Li_6PS_5Cl-layer on active material. Li_6PS_5Cl powder was dissolved in a mixture of ethanol (99.5%, Wako Pure Chemical, Japan) and

acetonitrile (99.5%, Wako Pure Chemical, Japan), the concentration of Li_6PS_5Cl solution was 0.1 g mL^{-1}. After complete dissolution of the solid electrolyte, adequate content of triton X100 solution (dissolved in acetonitrile) was added by dropping to Li_6PS_5Cl-solution.

Crystal phase, morphology and ionic conductivity of the Li_6PS_5Cl solid electrolyte obtained by mechanical milling and dissolution-reprecipitation process were examined to elucidate the effect of the solvent and dispersants on the properties of the sulfide electrolyte. Crystal phase evaluated by X-ray diffraction (XRD) was carried out with an X-ray diffractometer (MultiFlex600, Rigaku) using CuKα radiation. The ionic conductivity of pelletized samples was determined by electrochemical impedance spectroscopy (EIS) using an impedance analyser (SI 1260, Solartron) in a frequency range of 1 and 1×10^6 Hz at room temperature. The solid electrolyte powders (Approximately 120 mg) were pressed under 360 MPa (at room temperature) in a polycarbonate tube, 10 mm of diameter and two stainless steel (SS) disks were used as current collectors. Morphology of the Li_6PS_5Cl solid electrolyte powders were observed by scanning electron microscopy (SEM), performed on a JIB-4600F Multibeam SEM-FIB Scanning Electron Microscope without exposure to air.

The synthesis of the composite cathodes and the assembly of the cells were conducted in a glove box under an argon atmosphere. The composite cathodes were prepared using $LiNbO_2$-coated $LiNi_{1/3}Mn_{1/3}Co_{1/3}O_2$ (NMC) [20, 21], Li_6PS_5Cl solid electrolyte and vapor growth carbon fiber (VGCF, Showa Denko, Japan) as the

active material, ionic and conductive additives, respectively. Ethanol and acetonitrile were used as solvents. Triton X100 (Wako Pure Chemical) was used as a dispersant. The weight ratios NMC:Li_6PS_5Cl:VGCF of 84:14:2 and 89:9:2 were evaluated. The dispersant effect of 0.1 – 0.5 wt% were evaluated.

The composite cathode was prepared by solution process dispersing NMC and VGCF in the Li_6PS_5Cl-solution. A vortex mixer at 2800 RPM (AS ONE test tube shakers, Japan) was used to homogenize the slurry and the solvents were then removed by heating at 150 ºC (3h) or 180 ºC (3h) under vacuum. Morphology and compositional distribution of the prepared composite cathode were studied by SEM-EDS analysis.

Cell assembly and electrochemical measurements

All-solid-state batteries were constructed using $80Li_2S{\cdot}20P_2S_5$ (mol%) glass and In metal (99.99% 0.1 mm thickness) as solid electrolyte and anode, respectively. The $80Li_2S{\cdot}20P_2S_5$ solid electrolyte was prepared by mechanical milling using 1 g of stoichiometric proportions of Li_2S and P_2S_5 and 4 mm diameter zirconia balls (500 balls) in a zirconia pot (45 mL) at 510 RPM for 10 h. The composite cathode (10 mg) and the solid electrolyte powder (80 mg) were pressed under 360 MPa in a polycarbonate tube (ϕ= 10 mm). The indium metal (40 mg) was pressed under 240 MPa on the prepared pellet. The three-layered pellet was sandwiched between two stainless-steel disks as current collectors to fabricate two electrode cells. The electrochemical performance of the cell was evaluated under a constant current

density of 0.13 mA cm^{-2} in the voltage range from 2.0 V to 3.8 V vs. Li-In at room temperature, using a charge discharge measuring device (Scribner Associates, 580 battery type system).

Results and Discussion

Figure 1 shows the X-ray diffraction (XRD) patterns of the Li_6PS_5Cl solid electrolyte obtained by mechanical milling and dissolution-reprecipitation process. The XRD patterns of the Li_6PS_5Cl solid electrolyte obtained at two different temperatures, 150 °C and 180 °C, were included. In addition, XRD patterns of Li_6PS_5Cl solid electrolyte obtained from the SSE-solution containing 0.1 wt% and 0.5 wt% of dispersant were also included. Indexed XRD pattern of the $Li_{6.2}PS_5Cl$ (ICDD#418490) phase is shown for comparison. The XRD pattern of the powder obtained by mechanical milling displays the formation of the Li_6PS_5Cl phase. After dissolution-reprecipitation process at 150 °C, a complex XRD pattern was obtained. Peaks 2θ around 15º, 18º, 25º, 30º and 31 º are related with argyrodite phase while intense peaks 2θ around 27º and 35º can be attributed to Li_2S and LiCl phases, respectively. The other peaks could not be indexed by the structure of argyrodite or the starting precursor materials. Heat treatment at 180 °C was high enough to obtain well crystallized Li_6PS_5Cl phase and the full removal of solvent (additional reflections), sharper peaks indicate a high crystallinity than that obtained by mechanical milling. The addition of dispersant does not show significant change in the crystal Li_6PS_5Cl phase. The diffraction observed in the sample dried at 150 °C

have also been detected in other sulfide electrolytes prepared by liquid phase, associated to the formation of complex between solid electrolyte and solvents [19]. The presence of Li_2S and LiCl phases suggest their partial dissolution from argyrodite structure, however at 180 °C precursors changed in to the argyrodite structure. The XRD results indicate than Li_6PS_5Cl crystal phase can be obtained by dissolution-reprecipitation process with or without dispersants.

Figure 2 displays the morphology of the Li_6PS_5Cl solid electrolyte obtained by mechanical milling and dissolution-reprecipitation process. Morphology of Li_6PS_5Cl obtained from the SSE-solution containing 0.1 wt% and 0.5 wt% of dispersant were also included. Big particles with an irregular size range between 1 µm up to 20 µm were observed in the Li_6PS_5Cl solid electrolyte obtained by mechanical milling (Figure a). After dissolution-reprecipitation process at 180 °C, Li_6PS_5Cl particles derived from SSE-solution without dispersant (Figure 2b) shows smaller particles with irregular size from nanometers to 5 µm; while a regular distribution of the particles in nanometric scale with spherical shape, below 500 nm, are obtained from Li_6PS_5Cl particles derived from SSE-solution containing dispersant (Figure 2c-d). Smaller sized particles at nanometric scale around 100 nm were obtained by high content of dispersant (Figure 2e-f), however, agglomeration of particles was observed.

The particle size of Li_6PS_5Cl particles derived from SSE-solution is more than 10 times smaller compared with the particle size obtained by mechanical milling process.

The expected smaller particle size obtained by dissolution-reprecipitation process using acetonitrile and ethanol as medium solution, is attribute to the surfactant role of the acetonitrile [18, 22, 23]. In addition, the use of the dispersant leads not only to a smaller particle size but also to a regular size distribution of the particles. The dispersant adsorption during nucleation and particle formation allowed the control of particle size and prevented their aggregation during solvent removal.

Figure 3 shows the impedance plot at room temperature of Li_6PS_5Cl obtained by the dissolution-reprecipitation process without and with 0.1 wt% dispersant. Nyquist plot shows only a capacitive tail at high frequencies, which is attributed to the contribution of the interface between the ionic conductor and blocking stainless steel electrodes. The resistance of Li_6PS_5Cl was determined by the value of Z' at the intercept with the real axis obtained by linear fit. The ionic conductivity of the Li_6PS_5Cl derived from SSE-solution without dispersant attained 0.3×10^{-3} S cm^{-1} (ρ = 1.43 g cm^{-3}), while those containing dispersant achieved 0.6×10^{-3} S cm^{-1} (ρ = 1.40 g cm^{-3}). A higher amount of dispersant of 0.5 wt% (not shown) lead to a drop of conductivity of 0.2×10^{-3} S cm^{-1} (ρ = 1.38 g cm^{-3}).

The ionic conductivity of the Li_6PS_5Cl obtained by dissolution-reprecipitation process was one order of magnitude higher than that as-synthetized Li_6PS_5Cl by mechanical milling (0.4×10^{-4} S cm^{-1}) when used to prepare the SSE-solution. Li_6PS_5Cl derived from SSE-solution containing dispersant achieved the same value reported for Li_6PS_5Cl obtained by mechanical milling crystalized at 550 ºC (1×10^{-3} S cm^{-1} [24,

25]). These results suggest than the conductivity of sulfide solid electrolyte can be improved by the liquid phase process. The adequate selection of solvents and dispersants can reach values as high as those reported by high crystallized samples obtained by mechanical milling and heat treatments at high temperature. The improvement of the conductivity is attributed to the better particle size distribution of the Li_6PS_5Cl derived from solution containing dispersant, confirmed by SEM (Figure 2c-f). Although, the high crystallinity (verified by XRD, Figure 1) of the Li_6PS_5Cl obtained by liquid phase process makes pelletizing difficult, the particle distribution (size and shape) can mitigate this effect, improving the densification and therefore the ionic conductivity by reducing the grain boundary resistance. Addition of a larger dispersant amount lead to a decreasing of conductivity of the solid electrolyte cause by the insulator nature of the polymeric structure.

The conductivity of Li_6PS_5Cl solid electrolyte derived from solution using acetonitrile and ethanol as solvents is higher than other argyrodite-type prepared by liquid phase process using solvents such as ethanol[15, 16] (Li_6PS_5Cl, 0.2 x 10^{-4} S cm^{-1}) or mixture of the solvents ethyl propionate and ethanol[14] (Li_6PS_5Br, 0.3 x 10^{-4} S cm^{-1}). The difference, up to one order of magnitude, can be attributed to the different reactivity of each solvent with the sulfide electrolyte. The high conductivity of Li_6PS_5Cl reported in this work is comparable with other high conductor sulfide electrolytes prepared by liquid phase using acetonitrile [26, 27] such as $Li_7P_3S_{11}$ (1 x 10^{-3} S cm^{-1}). The results confirm that the acetonitrile is suitable as an organic medium for the formation of high conductor sulfide solid electrolytes obtained by

liquid phase process. Moreover, the result indicates that particle size of the sulfide solid electrolyte can be modified by liquid phase process using adequate dispersants without degradation of their chemical or electrochemical properties. A chemical route to control the particle size and shape of sulfide solid electrolyte by means of the use of dispersant agents is a promising route as this can prevent the chemical degradation produced by several multistage grindings obtained by a typical mechanical milling process [28].

Figure 4 displays SEM images of NMC particle without (used as reference) and with Li_6PS_5Cl-layer obtained by liquid phase process containing 0.1 wt% dispersant. Weight ratio between NMC and Li_6PS_5Cl is 89:9. Backscattering image (BS) and elemental composition mapping of manganese, sulfur, phosphorus and chlorine obtained by EDS are also shown. The SEM image of NMC (Figure 4a) shows the morphology of the typical particles, a hemispherical primary particle with overlapped secondary particles with a total size around 5 μm. The SEM image of NMC coated with Li_6PS_5Cl-layer (Figure 4b) shows a smooth surface morphology; smaller spherical particles around 100 nm were observed on surface of NMC particles. The Li_6PS_5Cl-layer were evidenced by the darker region on the BS image (Figure 4c). The BS image clearly displays the NMC morphology below Li_6PS_5Cl-layer. In addition, EDS mapping (Figure 4d-g) of elements from the sulfide solid electrolyte were homogenously detected on the surface of NMC particles, verifying the formation of Li_6PS_5Cl-layer on NMC particles. For comparison, Figure S1 shows similar SEM analysis of NMC particle with Li_6PS_5Cl-layer obtained by liquid phase

process without dispersant. The formation of Li_6PS_5Cl-layer on NMC was verified by BS image (Figure S1b) and EDS mapping (Figure S1c-f), however, bigger irregular particles of Li_6PS_5Cl with a size around 1 µm were observed.

SEM-EDS analysis of composite cathode obtained by liquid phase reveals that this process is effective to cover the surface of NMC particles, even with a very low content of Li_6PS_5Cl-layer (9 wt%). The observation also showed that the dispersant improved the precipitation of the Li_6PS_5Cl particles resulting in a better distribution of Li_6PS_5Cl-layer on NMC particles.

Figure 5 shows charge-discharge curves and cycle performance of the bulk-type ASLB cell fabricated with composite cathode prepared by the liquid phase process without dispersant. The composite cathode contains a relatively low content of Li_6PS_5Cl-layer of 14 wt%. The all-solid-state cell was evaluated in a voltage range of 2 V to 3.8 V (*vs.* Li-In) at a current density of 0.13 mA cm^{-2} at 25 °C. The cell works as a rechargeable battery achieving an initial discharge capacity of 140 mA h g^{-1} and capacity retention of ~80% after 25 cycles with a capacity efficiency of 100%. The discharge capacity decay during the first three cycles, however, subsequent cycles demonstrate much less capacity loss around 120 mA h g^{-1}.

Figure 6 shows initial charge-discharge curves and cycle performance of the bulk-type ASLB cells fabricated with composite cathodes prepared by the liquid phase process without and with different amount of dispersant. The composite cathode was prepared with a very low amount of Li_6PS_5Cl-layer of 9 wt%. The ASLB cells

prepared with composite cathode derived from solution without and with dispersant work as a rechargeable battery achieving an initial discharge capacity of 40 mA h g^{-1} and 115 mA h g^{-1} (0.25 wt% dispersant), respectively. Capacity retention of ~95% after 15 cycles with a capacity efficiency of 100% was determined for ASLB cell containing 0.1 wt% dispersant. Figure 7 shows cycle performance under higher current densities of ASSBs cells fabricated with composite cathode derived from Li_6PS_5Cl (9 wt%) precursor solution containing dispersant. After 75 cycles, the cells achieve a high discharge capacity of 95 mA h g^{-1} (0.1 wt% dispersant) with a capacity efficiency of 100%. The rate capabilities for the composite cathode was slightly enhanced by decreasing the amount of dispersant, which is attributed to improved ionic contact between Li_6PS_5Cl-layer and NMC. The larger amount of dispersant can reduce the ionic contact because of its non-ionic nature. High initial discharge capacity with enhanced rate capability can be obtained using dispersant amounts as small as 0.1 wt%, which is effective even during several cycles (Figure S2).

The high initial discharge capacity (140 mA h g^{-1}) of the bulk-type ASLB cell with a composite cathode containing 14 wt% Li_6PS_5Cl-layer prepared from solution without dispersant indicates that the Li_6PS_5Cl-layer is well formed facilitating an adequate ionic conduction pathway to the active material. However, when the content of Li_6PS_5Cl-layer is reduced to 9 wt% in the composite cathode, lower initial discharge capacity (40 mA h g^{-1}) is obtained. Although the liquid phase process facilitated by acetonitrile/ethanol solution is effective to prepare suitable electrode and electrolyte interface (low resistance) with relative low SSE content, new chemistries are needed

to promote better interfaces between NMC and Li_6PS_5Cl for composite cathode with reduced SSE amount (<10 wt%).

ASLB cells fabricated with the composite cathodes with 9 wt% Li_6PS_5Cl-layer prepared by liquid phase process containing dispersant shows an improved initial discharge capacity reaching 115 mA h g^{-1}, corresponding to more than double of the ASLB cell fabricated with composite cathodes derived from solution without dispersant. The results indicate that favorable electrolyte/electrode interface with intimate ionic pathway can be controlled by chemical way through strategic selection of protic/aprotic solvent and dispersant. During composite cathode preparation, the control of the precipitation of Li_6PS_5Cl-layer on NMC particles is assisted by the dispersant, therefore the dispersant lead to a suitable distribution of the SSE-layer on the active material (verified by SEM-EDS analysis, Figure 4) and good electrochemical performance.

The high conductivity of Li_6PS_5Cl-layer, estimated to be around 10^{-3} – 10^{-4} S cm^{-1}, is also considered to be a key fact for the enhanced low interface resistance and adequate electrochemical performance of the ASLB cells fabricated with composite cathodes with low Li_6PS_5Cl-layer amounts. The initial discharge capacity obtained from ASLB cells fabricated with the composite cathodes reported in this work, both with 9 wt% and 14 wt% Li_6PS_5Cl-layer, are higher than that reported for other composite cathodes prepared by liquid phase process with similar low SSE-layer content [12-16]. The nanostructuring of sulfide solid electrolyte in composite cathode

with low content of SSE (10 wt%) [17] has proven to be effective to produce better electrode/electrolyte interface with an initial discharge capacity of 130 mA h g^{-1} and 85% of capacity retention after 10 cycles. In this work, the control of the precipitation of sulfide solid electrolyte using dispersant during composite cathode preparation leads not only to high initial discharge capacity, but also to better capacity retention of 95% after 15 cycles. The result indicates that favorable SSE-layer on active material can be controlled by chemical way through strategic selection of protic/aprotic solvents with compatible dispersant.

Conclusions

Li_6PS_5Cl sulfide electrolyte with high conductivity (10^{-3} – 10^{-4} S cm^{-1}) can be obtained from dissolution-reprecipitation process through a strategic selection of protic/aprotic solvents and dispersant. Particle size and shape of sulfide solid electrolyte can be modified using dispersants without degradation of their chemical or electrochemical properties. Results of Li_6PS_5Cl-layer on NMC particles prepared by liquid phase process showed efficiency in improving the interfacial electrode/electrolyte resistance in bulk-type ASLB. The use of dispersants has proven to be effective to improving the total discharge capacity, capacity efficiency and cycle retention of the all-solid-state battery with high content of active material up to 89 wt%. Bulk-type ASLB fabricated with the composite cathode prepared by liquid phase process containing dispersant achieved 110 mAh g^{-1} with a capacity retention of 95% after 15 cycles.

Acknowledgements

The present work was supported by the Japan Science and Technology Agency (JST), Advanced Low Carbon Technology Research and Development Program (ALCA), and Specially Promoted Research for Innovative Next Generation Batteries (SPRING) project. The analysis of SEM was carried out with JIB4600F at the “Joint-use Facilities: Laboratory of Nano-Micro Material Analysis”, Hokkaido University, supported by “Material Analysis and Structure Analysis Open Unit (MASAOU)”.

References

[1] J.C. Bachman, S. Muy, A. Grimaud, H.H. Chang, N. Pour, S.F. Lux, O. Paschos, F. Maglia, S. Lupart, P. Lamp, L. Giordano, Y. Shao-Horn, Inorganic solid-state electrolytes for lithium batteries: mechanisms and properties governing ion conduction. Chem. Rev., 116 (2016) 140-162.

[2] A. Sakuda, H. Kitaura, A. Hayashi, K. Tadanaga, M. Tatsumisago, Improvement of high-rate performance of all-solid-state lithium secondary batteries using $LiCoO_2$ coated with Li_2O-SiO_2 glasses. Electrochemical and Solid State Letters, 11 (2008) A1-A3.

[3] J. Auvergniot, A. Cassel, J.B. Ledeuil, V. Viallet, V. Seznec, R. Dedryvere, Interface Stability of Argyrodite Li_6PS_5Cl toward $LiCoO_2$, $LiNi_{1/3}Co_{1/3}Mn_{1/3}O_2$, and $LiMn_2O_4$ in Bulk All-Solid-State Batteries. Chemistry of Materials, 29 (2017) 3883-3890.

[4] G. Oh, M. Hirayama, O. Kwon, K. Suzuki, R. Kanno, Bulk-Type All Solid-State Batteries with 5 V Class $LiNi_{0.5}Mn_{1.5}O_4$ Cathode and $Li_{10}GeP_2S_{12}$ Solid Electrolyte. Chemistry of Materials, 28 (2016) 2634-2640.

[5] Q. Zhang, J.P. Mwizerwa, H.L. Wan, L.T. Cai, X.X. Xu, X.Y. Yao, Fe_3S_4@$Li_7P_3S_{11}$ nanocomposites as cathode materials for all-solid-state lithium batteries with improved energy density and low cost. J. Mater. Chem. A., 5 (2017) 23919-23925.

[6] A. Hayashi, A. Sakuda, M. Tatsumisago, Development of Sulfide Solid Electrolytes and Interface Formation Processes for Bulk-Type All-Solid-State Li and Na Batteries. Frontiers in Energy Research, 4 (2016).

[7] G. Bucci, T. Swamy, Y.M. Chiang, W.C. Carter, Modeling of internal mechanical failure of all-solidstate batteries during electrochemical cycling, and implications for battery design. J. Mater. Chem. A., 5 (2017) 19422-19430.

[8] A. Sakuda, A. Hayashi, T. Ohtomo, S. Hama, M. Tatsumisago, All-solid-state lithium secondary batteries using $LiCoO_2$ particles with pulsed laser deposition coatings of Li_2S–P_2S_5 solid electrolytes. J. Power Sources, 196 (2011) 6735-6741.

[9] Y. Ito, M. Otoyama, A. Hayashi, T. Ohtomo, M. Tatsumisago, Electrochemical and structural evaluation for bulk-type all-solid-state batteries using Li_4GeS_4-Li_3PS_4 electrolyte coating on LiCoO2 particles. J. Power Sources, 360 (2017) 328-335.

[10] S. Teragawa, K. Aso, K. Tadanaga, A. Hayashi, M. Tatsumisago, Liquid-phase synthesis of a Li_3PS_4 solid electrolyte using *N*-methylformamide for all-solid-state lithium batteries. J. Mater. Chem. A., 2 (2014) 5095-5099.

[11] K. Lee, S. Kim, J. Park, S.H. Park, A. Coskun, D.S. Jung, W. Cho, J.W. Choi, Selection of Binder and Solvent for Solution-Processed All-Solid-State Battery. J. Electrochem. Soc., 164 (2017) A2075-A2081.

[12] K.H. Park, D.Y. Oh, Y.E. Choi, Y.J. Nam, L.L. Han, J.Y. Kim, H.L. Xin, F. Lin, S.M. Oh, Y.S. Jung, Solution-processable glass LiI-Li_4SnS_4 superionic conductors for all-solid-state Li-ion batteries. Adv. Mater. (Weinheim, Ger.), 28 (2016) 1874-1883.

[13] Y.E. Choi, K.H. Park, D.H. Kim, D.Y. Oh, H.R. Kwak, Y.G. Lee, Y.S. Jung, Coatable Li_4SnS_4 Solid Electrolytes Prepared from Aqueous Solutions for All-Solid-State Lithium-Ion Batteries. Chemsuschem, 10 (2017) 2605-2611.

[14] S. Chida, A. Miura, N.C. Rosero-Navarro, M. Higuchi, N.H.H. Phuc, H. Muto, A. Matsuda, K. Tadanaga, Liquid-phase synthesis of Li_6PS_5Br using ultrasonication and application to cathode composite electrodes in all-solid-state batteries. Ceramics International, 44 (2017) 742.

[15] S. Yubuchi, S. Teragawa, K. Aso, K. Tadanaga, A. Hayashi, M. Tatsumisago, Preparation of high lithium-ion conducting Li_6PS_5Cl solid electrolyte from ethanol solution for all-solid-state lithium batteries. J. Power Sources, 293 (2015) 941-945.

[16] N.C. Rosero-Navarro, T. Kinoshita, A. Miura, M. Higuchi, K. Tadanaga, Effect of the binder content on the electrochemical performance of composite cathode using Li_6PS_5Cl precursor solution in an all-solid-state lithium battery. Ionics, 23 (2017) 1619-1624.

[17] N.H.H. Phuc, K. Morikawa, T. Mitsuhiro, H. Muto, A. Matsuda, Synthesis of plate-like Li_3PS_4 solid electrolyte via liquid-phase shaking for all-solid-state lithium batteries. Ionics, (2017) 1-7.

[18] H. Wang, Z.D. Hood, Y.N. Xia, C.D. Liang, Fabrication of ultrathin solid electrolyte membranes of β-Li_3PS_4 nanoflakes by evaporation-induced self-assembly for all-solid-state batteries. J. Mater. Chem. A., 4 (2016) 8091-8096.

[19] M. Calpa, N.C. Rosero-Navarro, A. Miura, K. Tadanaga, Instantaneous preparation of high lithium-ion conducting sulfide solid electrolyte $Li_7P_3S_{11}$ by a liquid phase process. RSC Adv., 7 (2017) 46499-46504.

[20] A. Sakuda, T. Takeuchi, H. Kobayashi, Electrode morphology in all-solid-state lithium secondary batteries consisting of $LiNi_{1/3}Co_{1/3}Mn_{1/3}O_2$ and Li_2S-P_2S_5 solid electrolytes. Solid State Ionics, 285 (2016) 112-117.

[21] N. Ohta, K. Takada, I. Sakaguchi, L.Q. Zhang, R.Z. Ma, K. Fukuda, M. Osada, T. Sasaki, $LiNbO_3$-coated $LiCoO_2$ as cathode material for all solid-state lithium secondary batteries. Electrochem. Commun., 9 (2007) 1486-1490.

[22] N.H.H. Phuc, K. Morikawa, M. Totani, H. Muto, A. Matsuda, Chemical synthesis of Li_3PS_4 precursor suspension by liquid-phase shaking. Solid State Ionics, 285 (2016) 2-5.

[23] X.Y. Yao, D. Liu, C.S. Wang, P. Long, G. Peng, Y.S. Hu, H. Li, L.Q. Chen, X.X. Xu, High-Energy All-Solid-State Lithium Batteries with Ultralong Cycle Life. Nano Lett., 16 (2016) 7148-7154.

[24] H.J. Deiseroth, S.T. Kong, H. Eckert, J. Vannahme, C. Reiner, T. Zaiß, M. Schlosser, Li_6PS_5X: a class of crystalline Li-rich solids with an unusually high Li^+ mobility. Angew. Chem., Int. Ed., 47 (2008) 755-758.

[25] C. Yu, L. van Eijck, S. Ganapathy, M. Wagemaker, Synthesis, structure and electrochemical performance of the argyrodite Li_6PS_5Cl solid electrolyte for Li-ion solid state batteries. Electrochimica Acta, 215 (2016) 93-99.

[26] R.C. Xu, X.H. Xia, Z.J. Yao, X.L. Wang, C.D. Gu, J.P. Tu, Preparation of Li7P3S11 glass-ceramic electrolyte by dissolution-evaporation method for all-solid-state lithium ion batteries. Electrochimica Acta, 219 (2016) 235-240.

[27] M. Calpa, N.C. Rosero-Navarro, A. Miura, K. Tadanaga, Preparation of sulfide solid electrolytes in the Li2S-P2S5 system by a liquid phase process. Inorganic Chemistry Frontiers, (2018).

[28] K. Sugiura, M. Ohashi, in: Method for producing sulfide solid electrolyte, Google Patents, 2014.

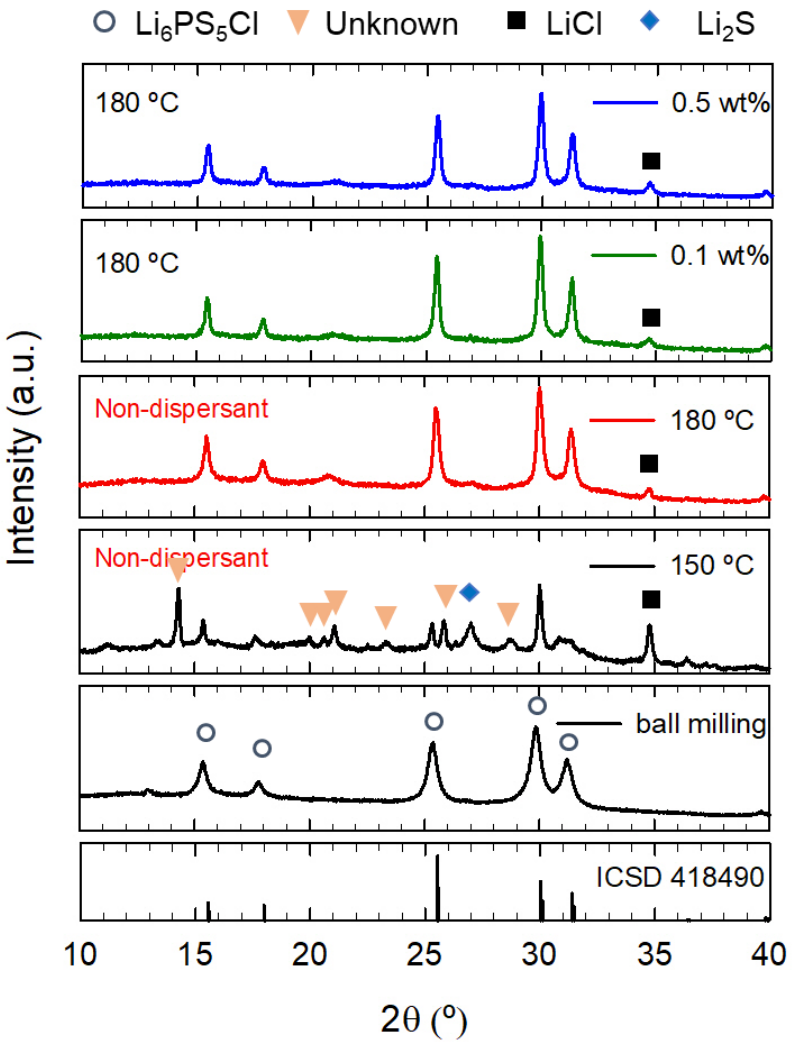

Figure 1. XRD of the Li_6PS_5Cl obtained by mechanical milling process and after dissolution-reprecipitation process at 150 ºC and 180 ºC. XRD patterns of Li_6PS_5Cl obtained from the SSE-solution containing 0.1 wt% and 0.5 wt% of dispersant are also included.

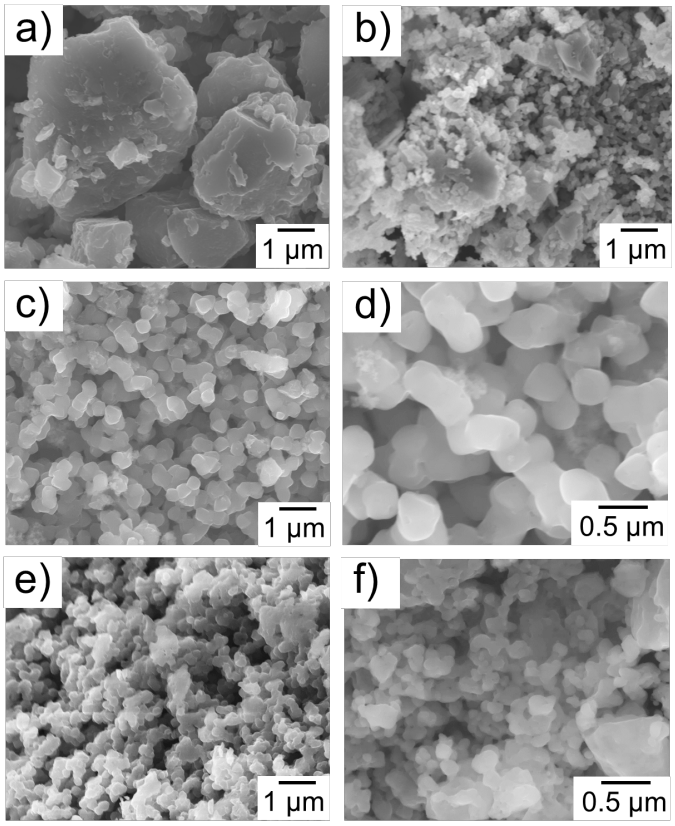

Figure 2. SEM of Li_6PS_5Cl solid electrolyte obtained by a) mechanical milling process and b) dissolution-reprecipitation process at 180 ˚C. Li_6PS_5Cl from the precursor solution containing c) - d) 0.1 wt% and e) - f) 0.5 wt% of dispersant.

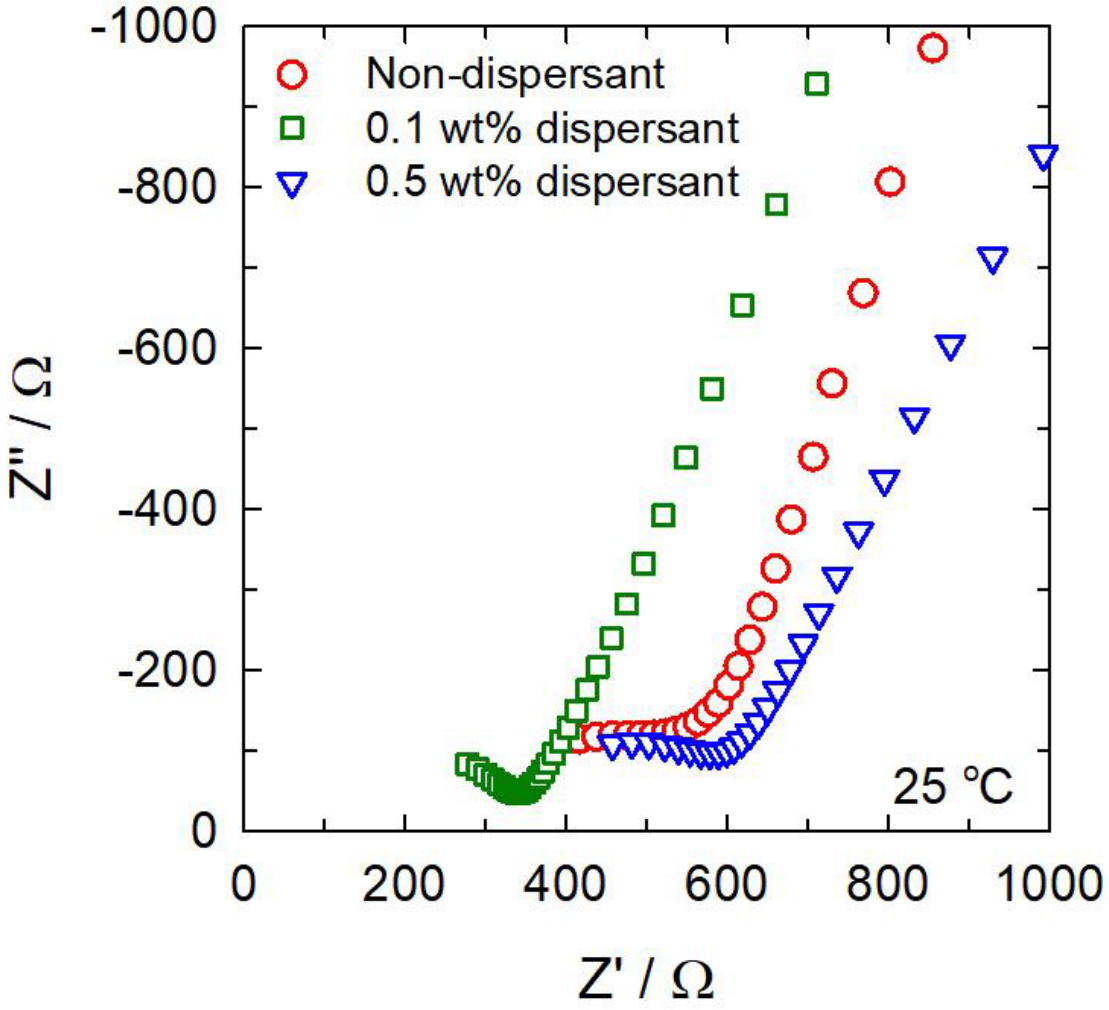

Figure 3. Nyquist plot of Li_6PS_5Cl solid electrolyte obtained by dissolution-reprecipitation process without and with dispersant.

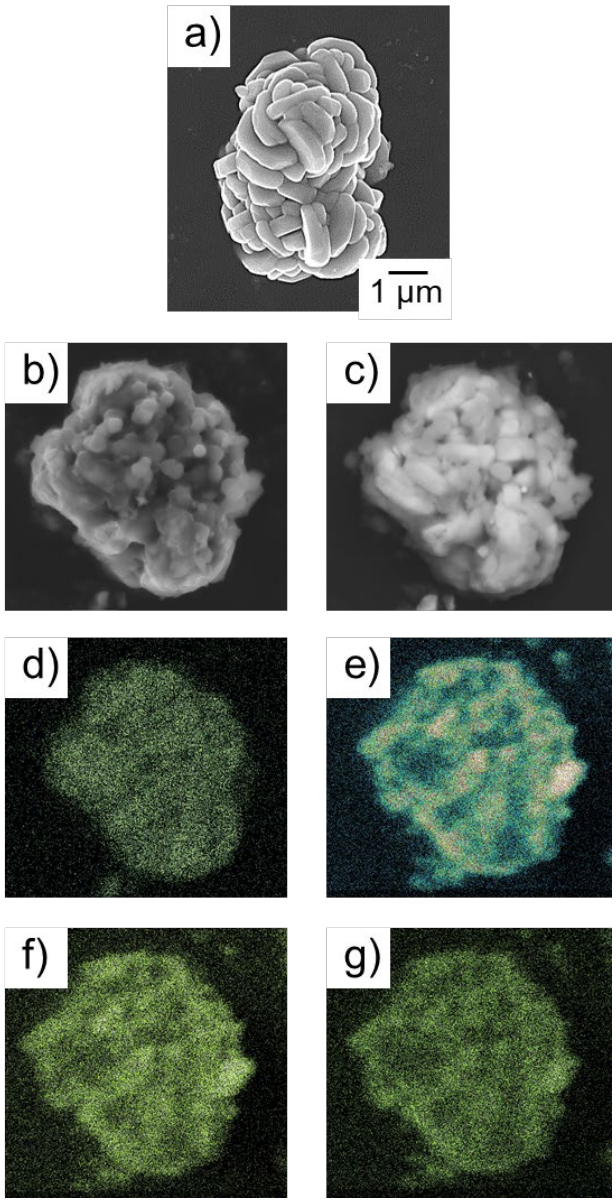

Figure 4. SEM morphology of NMC a) pristine particle and b) coated with Li_6PS_5Cl-layer from SSE-solution containing 0.1 wt% dispersant. c) Backscattering image and d)-g) EDS mapping of manganese, sulfur, phosphorus and chlorine, respectively. Weight ratio NMC:Li_6PS_5Cl of 89:9.

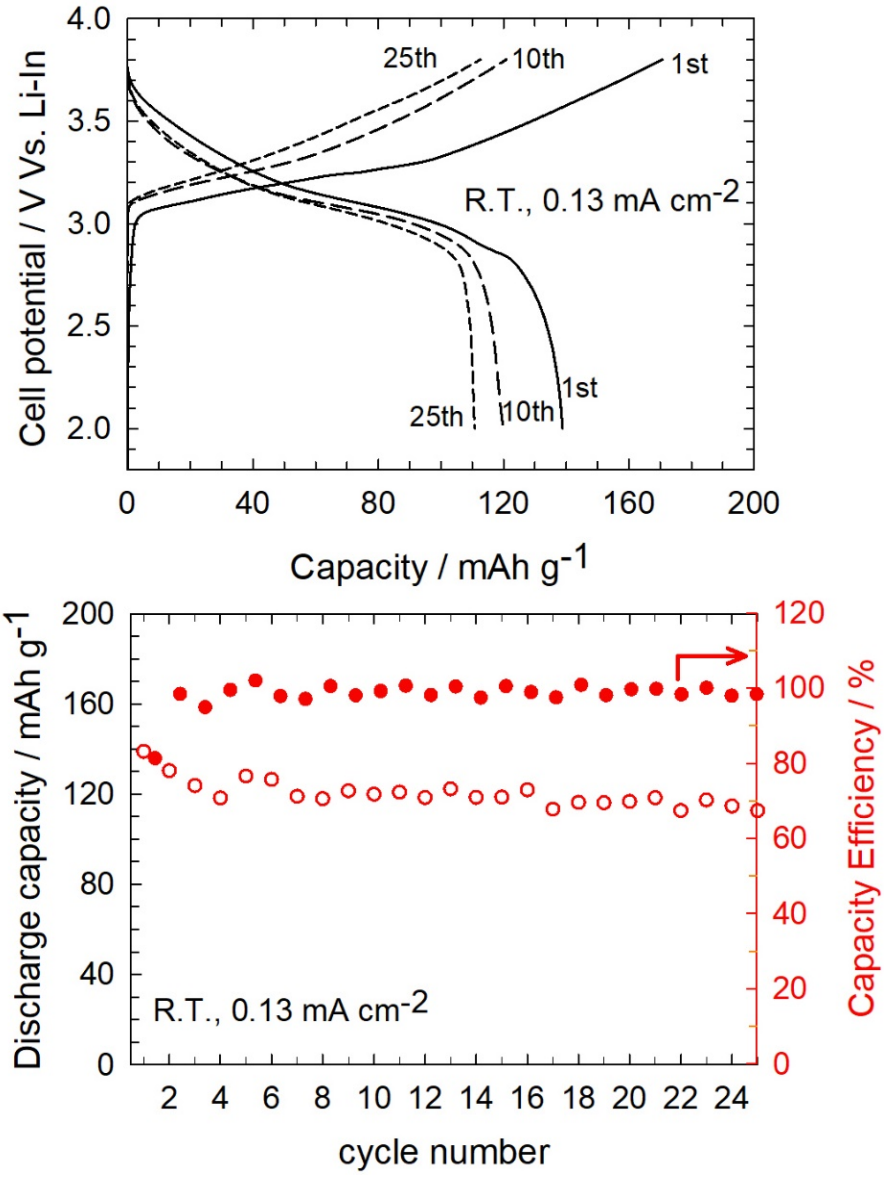

Figure 5. Charge-discharge (top) curves and cycle performances (bottom) of ASSB cell fabricated with composite cathode derived from Li_6PS_5Cl precursor solution without dispersant. Weight ratio composite NMC:Li_6PS_5Cl:VGCF of 84:14:2.

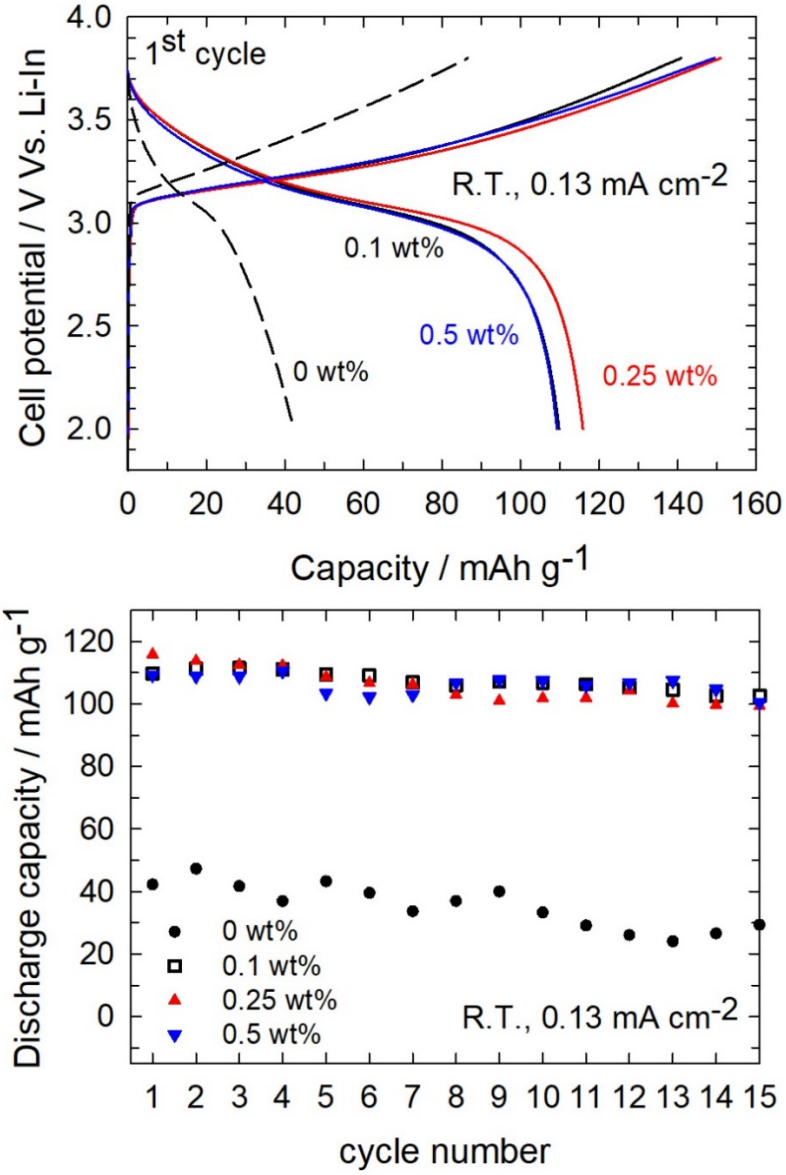

Figure 6. Charge-discharge (top) curves and cycle performances (bottom) of ASSBs cell fabricated with composite cathode derived from Li_6PS_5Cl precursor solution with and without dispersant. Weight ratio composite NMC:Li_6PS_5Cl:VGCF of 89:9:2.

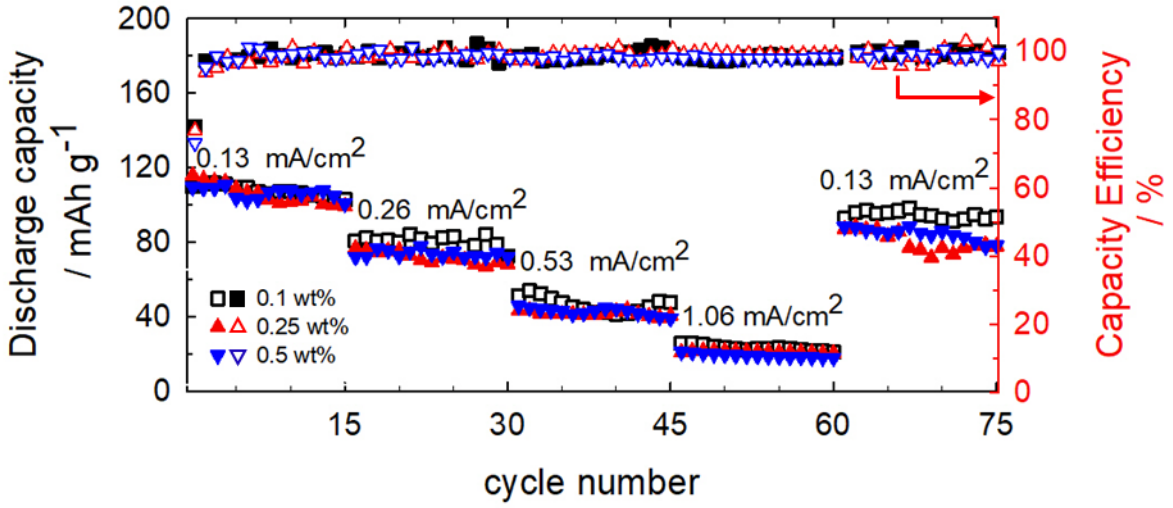

Figure 7. Cycle performances under higher current densities of ASSBs cell fabricated with composite cathode derived from Li_6PS_5Cl precursor solution containing dispersant. Weight ratio composite NMC:Li_6PS_5Cl:VGCF of 89:9:2.